

Prediction of coronary artery disease based on facial temperature information captured by non-contact infrared thermography

Minghui Kung,^{1,2} Juntong Zeng^{1,2},^{3,4,5} Shen Lin,^{3,4,5,6,7} Xuexin Yu,¹ Chang Liu,¹ Mengnan Shi,¹ Runchen Sun,^{3,4,5} Shangyuan Yuan,^{1,2} Xiaocong Lian,⁸ Xiaoting Su,^{3,4,5} Yan Zhao,^{3,4,6,7} Zhe Zheng^{1,2},^{3,4,5,6,7} Xiangyang Ji^{1,8}

To cite: Kung M, Zeng J, Lin S, *et al*. Prediction of coronary artery disease based on facial temperature information captured by non-contact infrared thermography. *BMJ Health Care Inform* 2024;**31**:e100942. doi:10.1136/bmjhci-2023-100942

► Additional supplemental material is published online only. To view, please visit the journal online (<https://doi.org/10.1136/bmjhci-2023-100942>).

MK, JZ, SL and XY contributed equally.

Received 19 October 2023
Accepted 06 March 2024



© Author(s) (or their employer(s)) 2024. Re-use permitted under CC BY-NC. No commercial re-use. See rights and permissions. Published by BMJ.

For numbered affiliations see end of article.

Correspondence to
Dr Zhe Zheng;
zhengzhe@fuwai.com

Dr Xiangyang Ji;
xyji@tsinghua.edu.cn

ABSTRACT

Background Current approaches for initial coronary artery disease (CAD) assessment rely on pretest probability (PTP) based on risk factors and presentations, with limited performance. Infrared thermography (IRT), a non-contact technology that detects surface temperature, has shown potential in assessing atherosclerosis-related conditions, particularly when measured from body regions such as faces. We aim to assess the feasibility of using facial IRT temperature information with machine learning for the prediction of CAD.

Methods Individuals referred for invasive coronary angiography or coronary CT angiography (CCTA) were enrolled. Facial IRT images captured before confirmatory CAD examinations were used to develop and validate a deep-learning IRT image model for detecting CAD. We compared the performance of the IRT image model with the guideline-recommended PTP model on the area under the curve (AUC). In addition, interpretable IRT tabular features were extracted from IRT images to further validate the predictive value of IRT information.

Results A total of 460 eligible participants (mean (SD) age, 58.4 (10.4) years; 126 (27.4%) female) were included. The IRT image model demonstrated outstanding performance (AUC 0.804, 95% CI 0.785 to 0.823) compared with the PTP models (AUC 0.713, 95% CI 0.691 to 0.734). A consistent level of superior performance (AUC 0.796, 95% CI 0.782 to 0.811), achieved with comprehensive interpretable IRT features, further validated the predictive value of IRT information. Notably, even with only traditional temperature features, a satisfactory performance (AUC 0.786, 95% CI 0.769 to 0.803) was still upheld.

Conclusion In this prospective study, we demonstrated the feasibility of using non-contact facial IRT information for CAD prediction.

INTRODUCTION

Coronary artery disease (CAD) is the leading cause of mortality and imposes a significant disease burden worldwide.¹ Accurate CAD assessment is crucial to inform appropriate downstream care. Current guidelines

WHAT IS ALREADY KNOWN ON THIS TOPIC

- ⇒ The current conventional approaches for initial coronary artery disease (CAD) assessment in clinical practice mainly rely on pretest probability tools based on traditional risk factors and symptoms, which often exhibit limited prediction performance.
- ⇒ Infrared thermography (IRT), a non-contact technology that captures surface temperature, has shown promising potential in assessing various atherosclerosis-related conditions but has not yet been evaluated for its clinical feasibility in predicting CAD.

WHAT THIS STUDY ADDS

- ⇒ For suspected individuals referred for confirmatory CAD evaluation, we demonstrated that human facial temperature information captured by the non-contact IRT can be effectively used by advanced machine learning algorithms for predicting CAD.
- ⇒ Both an end-to-end, deep-learning-based facial IRT image analysis approach and an interpretable facial temperature variable extraction approach exhibited superior performance for CAD prediction, compared with conventional clinical methods.

HOW THIS STUDY MIGHT AFFECT RESEARCH, PRACTICE OR POLICY

- ⇒ Novel biophysiological information from facial temperature offers the possibility of real-time, non-contact CAD detection, which could potentially be adopted in clinical practice to improve the accuracy of CAD assessment and optimise the current clinical workflow.

rely on pretest probability (PTP) tools to estimate CAD probability in suspected patients.^{2,3} However, these tools suffer from issues of subjectivity, modest precision and limited generalisability.³⁻⁵ Although supplementary cardiovascular examinations such as electrocardiography and coronary artery calcium (CAC) score, or complex clinical models incorporating additional risk factors

of comorbidities and laboratory markers, could improve CAD probability estimation, they often present challenges regarding procedural complexity, time efficiency and limited availability.^{6–10} Therefore, there is a need for more accurate CAD prediction tools that efficiently integrate these different aspects of additional CAD-related information.

Infrared thermography (IRT) is a non-contact, real-time imaging technology that captures temperature distribution and variations on the object's surface by detecting self-emitted infrared radiation.¹¹ This non-invasive approach has emerged as a promising tool for disease assessment, as it can identify areas of abnormal blood circulation and inflammation activity through the measurement of skin temperature patterns. Studies in recent years have revealed strong associations between human body IRT temperature information and various conditions related to atherosclerotic cardiovascular disease (ASCVD), including carotid and peripheral artery diseases (PAD),^{12–13} diabetes,¹⁴ hyperlipidaemia,¹⁵ metabolic syndrome¹⁶ and inflammatory conditions.^{17–18} Among these studies, the human face has received particular attention due to its convenience and the previously reported link between human facial features and CAD risk.^{19–20} However, previous IRT studies have used simplistic, low-dimensional IRT information extracted and analysed with conventional statistical methods, which limited their ability to objectively and comprehensively quantify and use the wealth of information contained in IRT images. The advent of machine learning (ML) technology to extract, process and integrate complex information has shown impressive capability in harnessing the myriad of imaging information for various disease predictions.^{21–23} Therefore, we hypothesised that the IRT information measured from human faces, with the aid of ML technology, could be fully used for CAD prediction in a non-contact manner.

This study aims to investigate the feasibility of using non-contact captured facial IRT temperature information for CAD prediction.

METHODS

Study design and participants

This is a prospective, single-centre, cross-sectional study (ClinicalTrials.gov Identifier: NCT04941560). Eligible adult participants undergoing invasive coronary angiography (ICA) or coronary CT angiography (CCTA) at the National Center for Cardiovascular Disease, Fuwai Hospital were enrolled (detailed inclusion and exclusion criteria in online supplemental method S1). Informed consents were obtained from all eligible patients, with permission to use their facial IRT images, as well as required medical record data, for research-only deidentified analysis. Our study followed the Transparent Reporting of a Multivariable Prediction Model for Individual Prognosis or Diagnosis reporting guideline (online supplemental table S1).²⁴

Data collection

Trained clinical researchers collected baseline information and conducted IRT filming. The participants' presenting complaints, lifestyles, socioeconomic status, medical and family history, and medication usage were documented. The IRT filming was conducted in a confined room with air conditioning-controlled environmental temperature prior to the ICA or CCTA examination. Participants were seated in a stationary position, looking horizontally and naturally at an IRT camera (FLIR A315, FLIR Systems, USA) fixed at a distance of 1.5 m. The IRT filming commenced after proper positioning and alignment of the participant's face and a 3 min resting period. The entire filming process lasted for at least 5 s with the participant maintaining a still and centred position in the IRT capturing frame. Further demographic information, clinical history and risk factors, baseline blood biochemistry results and confirmatory CAD workup findings were obtained by reviewing participants' electronic medical records.

Data preparation and labelling

For each participant, one facial IRT image was selected and underwent preparation procedures before analyses, including greyscale conversion, background cropping and uniform resizing (online supplemental method S2). The prediction of interest in this study is the presence of CAD or not, as evidenced by ICA or CCTA findings, defined as a coronary lesion stenosis $\geq 50\%$. Two interventional cardiologists or radiologists, blinded to the study design and patient information, independently reviewed ICA or CCTA findings to evaluate the presence and/or degree of CAD lesions. Discrepancies were resolved through a third reviewer invited for final consensus.

Clinical and IRT image models for CAD prediction

To develop and evaluate CAD prediction models, we performed five repetitions of fivefold cross-validations with random shuffling.

- i. IRT image model: We employed an advanced deep-learning algorithmic framework optimised for relatively small-sample training while effectively leveraging relevant information to achieve satisfactory prediction performance. This framework comprises two essential components: the contrastive language-image pretraining image encoder, known for its exceptional zero-shot capabilities in extracting high-fidelity image features without task-specific training²⁵ and a vision transformer layer incorporating self-attention mechanisms to capture global context and relationships within the image for better integration of local and global features.²⁶ Additionally, a single fully connected layer served as the final classifier (detailed algorithm description and training process in online supplemental method S3; algorithm framework in online supplemental figure S1). This streamlined framework operated in an end-to-end manner for CAD prediction based on one single IRT image.

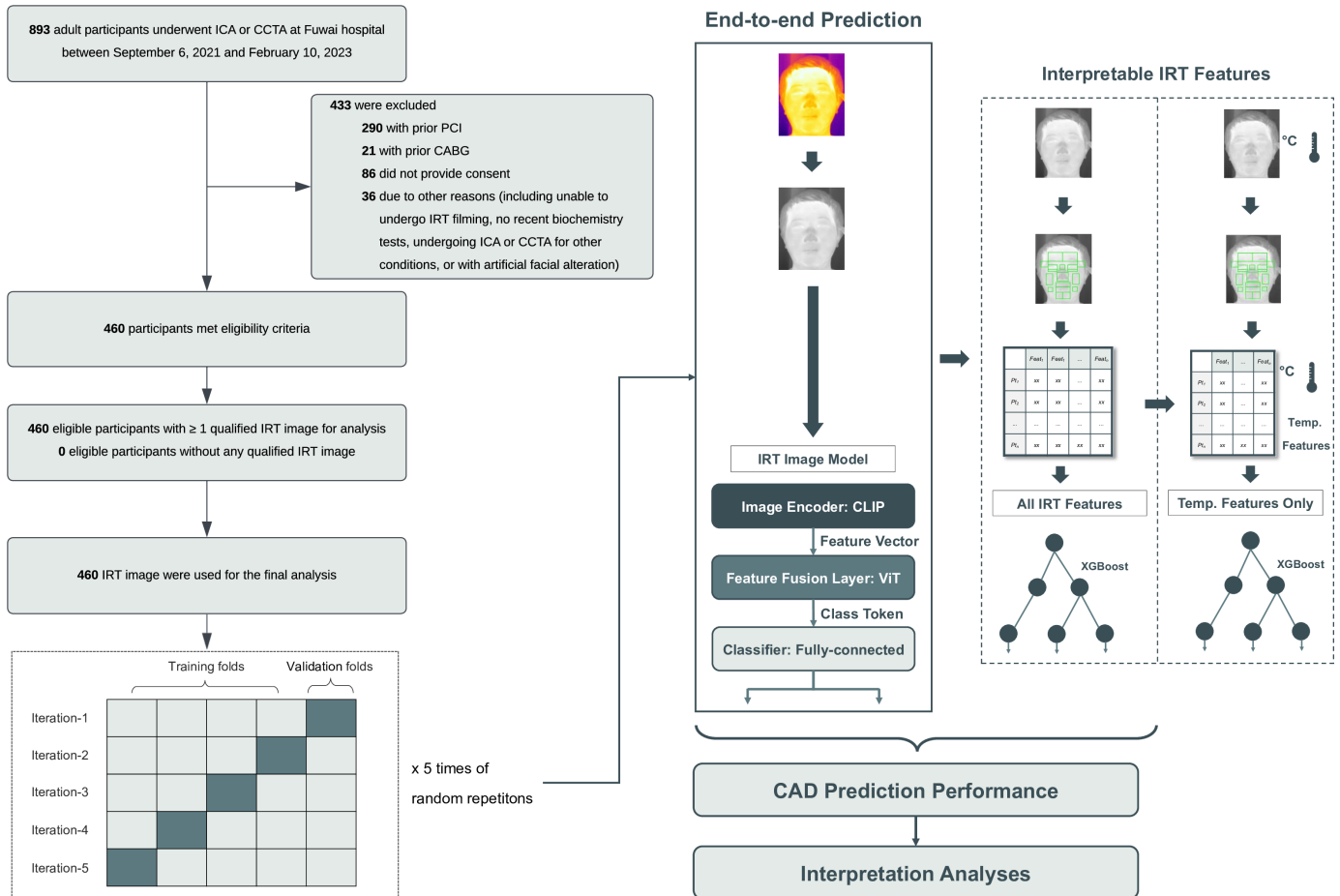


Figure 1 Flow chart of the study dataset and design. CABG, coronary artery bypass grafting; CAD, coronary artery disease; CCTA, coronary CT angiography; CLIP, contrastive language-image pretraining; ICA, invasive coronary angiography; IRT, infrared thermography; PCI, percutaneous coronary intervention; Temp., temperature; ViT, vision transformer.

- ii. Models with clinical variables: Two CAD prediction models with clinical information were constructed for comparison with the IRT image model. (1) The guideline-recommended PTP model for CAD prediction, which requires the patient’s age, sex and presenting symptom characteristics,^{3,7} served as the clinical baseline for predicting CAD. (2) A hybrid model that incorporated both clinical and IRT information. Specifically, this model fused the clinical variables from the PTP model with the IRT information from the IRT image model, in order to assess whether there was any additional performance improvement from this joint data input.

IRT image model interpretation

To enhance our understanding of how IRT information contributes to CAD prediction, we conducted a series of interpretation analyses to gain insights into the IRT image model:

- i. Occlusion experiments: To quantify the contribution of different IRT facial regions to model’s predictions, we sequentially occluded the corresponding region of interest (ROI) for each of the 10 facial regions. We then measured the individual impact of each occlusion on the model’s performance.

- ii. Saliency map visualisation: The gradient-weighted class activation map (Grad-CAM) method was employed to visually identify key areas in each facial IRT image that the algorithm focuses on for CAD prediction (online supplemental method S4).²⁷
- iii. Dose–response analyses: To explore the potential causal relationship between facial IRT information and CAD status, we investigated the association between individuals’ CAD risk predicted by the IRT model and the CAD lesion severity.
- iv. CAD surrogate label prediction: To further explore potential mechanisms by which IRT information may contribute to CAD prediction, we hypothesised that the IRT model’s predictive potential may derive from identifying various CAD-contributing or related aspects, represented by surrogate labels of ASCVD risk factors and other cardiovascular or inflammation markers. We tested this hypothesis by evaluating the performance of IRT models in predicting these surrogate labels.

Interpretable IRT features for CAD prediction

To further validate our hypothesis regarding the predictive value of IRT information for CAD and to obtain more human-interpretable insights, we extracted a diverse

Table 1 Baseline characteristics

	Overall (n=460)	CAD (n=322)	No CAD (n=138)	P value
Age, mean (SD)	58.4 (10.4)	60.4 (9.7)	53.8 (10.6)	<0.001
Female sex, n (%)	126 (27.4)	74 (23.0)	52 (37.7)	0.002
Smoking, n (%)	219 (47.6)	177 (55.0)	42 (30.4)	<0.001
BMI, mean (SD)	25.5 (3.0)	25.6 (3.0)	25.2 (3.0)	0.155
Menopause, n (%)	107 (84.9)	71 (95.9)	36 (69.2)	<0.001
Early ASCVD family history, n (%)	18 (3.9)	15 (4.7)	3 (2.2)	0.128
Hypertension, n (%)	267 (58.0)	215 (66.8)	52 (37.7)	<0.001
Hyperlipidaemia, n (%)	348 (75.7)	295 (91.6)	53 (38.4)	<0.001
Diabetes mellitus, n (%)	112 (24.3)	96 (29.8)	16 (11.6)	<0.001
Cerebrovascular event, n (%)	67 (14.6)	59 (18.3)	8 (5.8)	0.001
Peripheral artery disease, n (%)	48 (10.4)	44 (13.7)	4 (2.9)	0.001
Congestive heart failure, n (%)	63 (13.7)	32 (9.9)	31 (22.5)	0.001
Chronic kidney disease, n (%)	5 (1.1)	4 (1.2)	1 (0.7)	1.00
COPD, n (%)	7 (1.5)	5 (1.6)	2 (1.4)	1.00
Atrial Fibrillation, n (%)	35 (7.6)	21 (6.5)	14 (10.1)	0.250
Chronic inflammatory disease, n (%)	18 (3.9)	14 (4.3)	4 (2.9)	0.637
CAD symptoms, n (%)				
No symptoms	77 (16.7)	42 (13.0)	35 (25.4)	0.002
Non-anginal	102 (22.2)	70 (21.7)	32 (23.2)	
Atypical	146 (31.7)	102 (31.7)	44 (31.9)	
Typical	135 (29.3)	108 (33.5)	27 (19.6)	
Regular medications				
Aspirin, n (%)	191 (41.5)	173 (53.7)	18 (13.0)	<0.001
Beta blocker, n (%)	116 (25.2)	92 (28.6)	24 (17.4)	0.016
Statin, n (%)	210 (45.7)	173 (53.7)	37 (26.8)	<0.001
Nonstatin lipid-lowering drugs, n (%)	11 (2.4)	7 (2.2)	4 (2.9)	0.740
ACEI/ARB, n (%)	125 (27.2)	103 (32.0)	22 (15.9)	0.001
CCB, n (%)	121 (26.3)	94 (29.2)	27 (19.6)	0.042
Fast glucose, mean (SD)	6.3 (2.0)	6.5 (2.2)	5.7 (1.3)	<0.001
Total cholesterol, mean (SD)	4.3 (1.2)	4.2 (1.2)	4.7 (1.1)	<0.001
Triglyceride, mean (SD)	1.7 (1.7)	1.7 (1.9)	1.5 (0.9)	0.058
HDL, mean (SD)	1.2 (0.3)	1.2 (0.3)	1.3 (0.3)	<0.001
LDL, mean (SD)	2.5 (1.0)	2.4 (0.9)	2.9 (1.0)	<0.001
Haemoglobin A1c%, mean (SD)	6.3 (1.2)	6.4 (1.2)	5.9 (0.7)	<0.001
ESR, mean (SD)	8.0 (9.6)	8.3 (10.2)	6.7 (5.8)	0.069
CRP, mean (SD)	3.6 (5.2)	3.7 (5.5)	3.0 (3.4)	0.231
LVEF, mean (SD)	63.2 (6.2)	62.5 (6.6)	65.1 (4.5)	<0.001
Coronary confirmatory exam, n (%)				
ICA	379 (82.4)	310 (96.3)	69 (50.0)	<0.001
CCTA	81 (17.6)	12 (3.7)	69 (50.0)	
Coronary Lesion severity, n (%)				
No coronary stenosis >50%	138 (30.0)	/	138 (100.0)	<0.001
One vessel	89 (19.3)	89 (27.6)	/	
Two vessels	74 (16.1)	74 (23.0)	/	
Left main or three or more vessels	159 (34.6)	159 (49.4)	/	

ACEI/ARB, ACE inhibitor or angiotensin receptor blocker; ASCVD, atherosclerotic cardiovascular diseases; BMI, body mass index; CAD, coronary artery disease; CCB, calcium channel blocker; CCTA, coronary CT angiography; COPD, chronic obstructive pulmonary disease; CRP, C reactive protein; ESR, erythrocyte sedimentation rate; HDL, high-density lipoprotein; ICA, invasive coronary angiography; LDL, low-density lipoprotein; Lp(a), lipoprotein(a); LVEF, left ventricular ejection fraction.

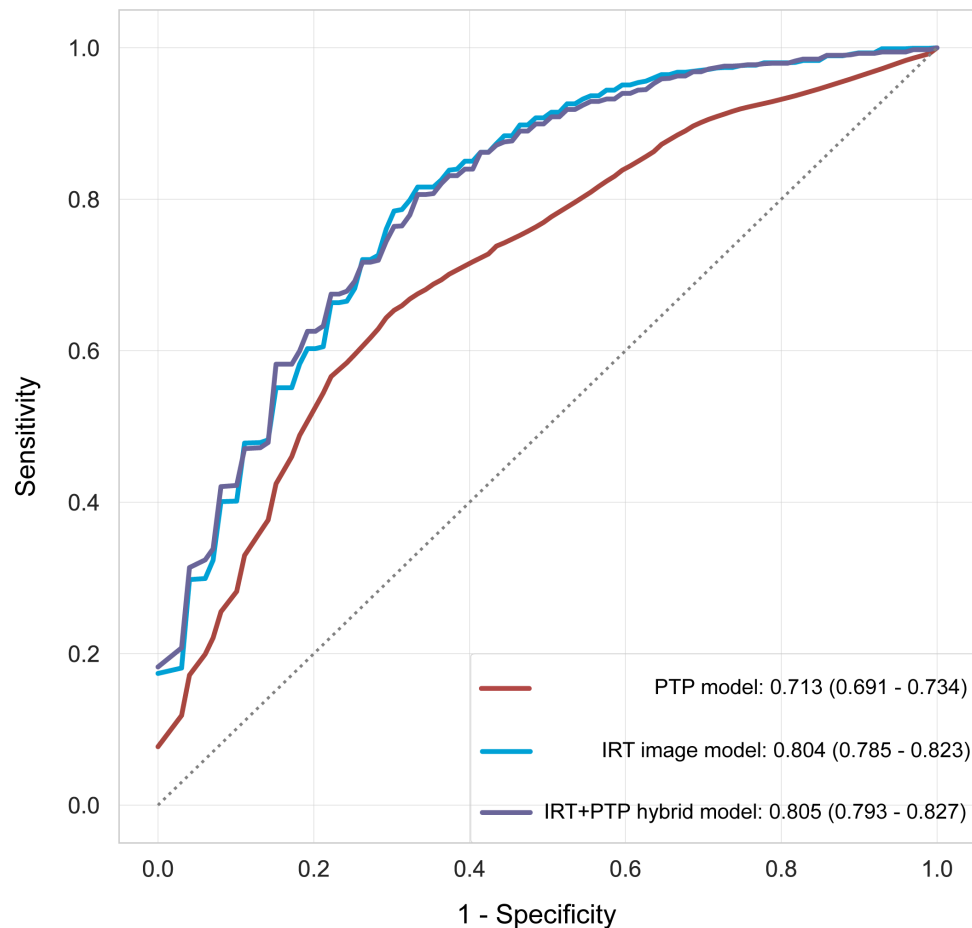


Figure 2 Receiver operating characteristic curves of models performance for CAD prediction. The legend in the right lower corner indicates different CAD prediction models and their corresponding AUC estimates, as well as the 95% CIs. AUC, area under the curve; CAD, coronary artery disease; IRT, Infrared thermography; PTP, pretest probability.

set of IRT tabular features from the IRT image. These features served as purer and more intuitive representations of underlying IRT information, reflecting facial temperature distribution. These extracted IRT features were categorised into two main levels: whole-face level and ROI-specific level. At the ROI-specific level, we partitioned the image into 18 facial ROIs (online supplemental method S5) and extracted features, respectively, resulting in a total of 619 ROI-specific IRT features. In addition, nine features were extracted at the whole-face level. A total of 628 IRT features encompassed four categories, namely: traditional temperature features, first-order texture features, second-order texture features and the fractal analysis feature (detailed description and a complete list of IRT features in online supplemental method S5 and table S2).

We employed the XGBoost algorithm, a gradient-boosted decision tree approach,²⁸ to integrate these extracted interpretable IRT features and assess their predictive values for CAD. We evaluated the performance of two approaches: one using all the interpretable IRT features and the other using only the traditional temperature features. The former comprehensive IRT feature approach aimed to approximate as much volume of IRT information as that used in the end-to-end IRT image

model. Whereas, the traditional temperature feature-only approach was to explore the predictive values of traditional temperature variables, which can be more readily available in clinical practice even if an IRT camera is not readily accessible. We further leveraged the feature importance functionality inherent in tree-based ML models to obtain rankings of individual facial IRT features, which assigned importance scores to each feature based on their contributions to the overall model performance.

Statistical analysis

Data are presented as mean with SD or median with IQR for continuous variables, and percentages for categorical variables. Student's t-test or Wilcoxon rank-sum test was used to compare continuous variables, while the χ^2 test or Fisher's exact test was used for categorical variables. The model's discrimination performance was evaluated by area under the curve (AUC) with 95% CIs. All comparisons were two sided, with statistical significance defined as $p < 0.05$, without adjustment for multiple comparisons. MATLAB V.R2021b (MathWorks, Massachusetts, USA) and Python V.3.10.5 were used for data preprocessing and model development, and R V.4.0.3 (R Foundation for Statistical Computing, Vienna, Austria) was used for plotting and statistical analysis.

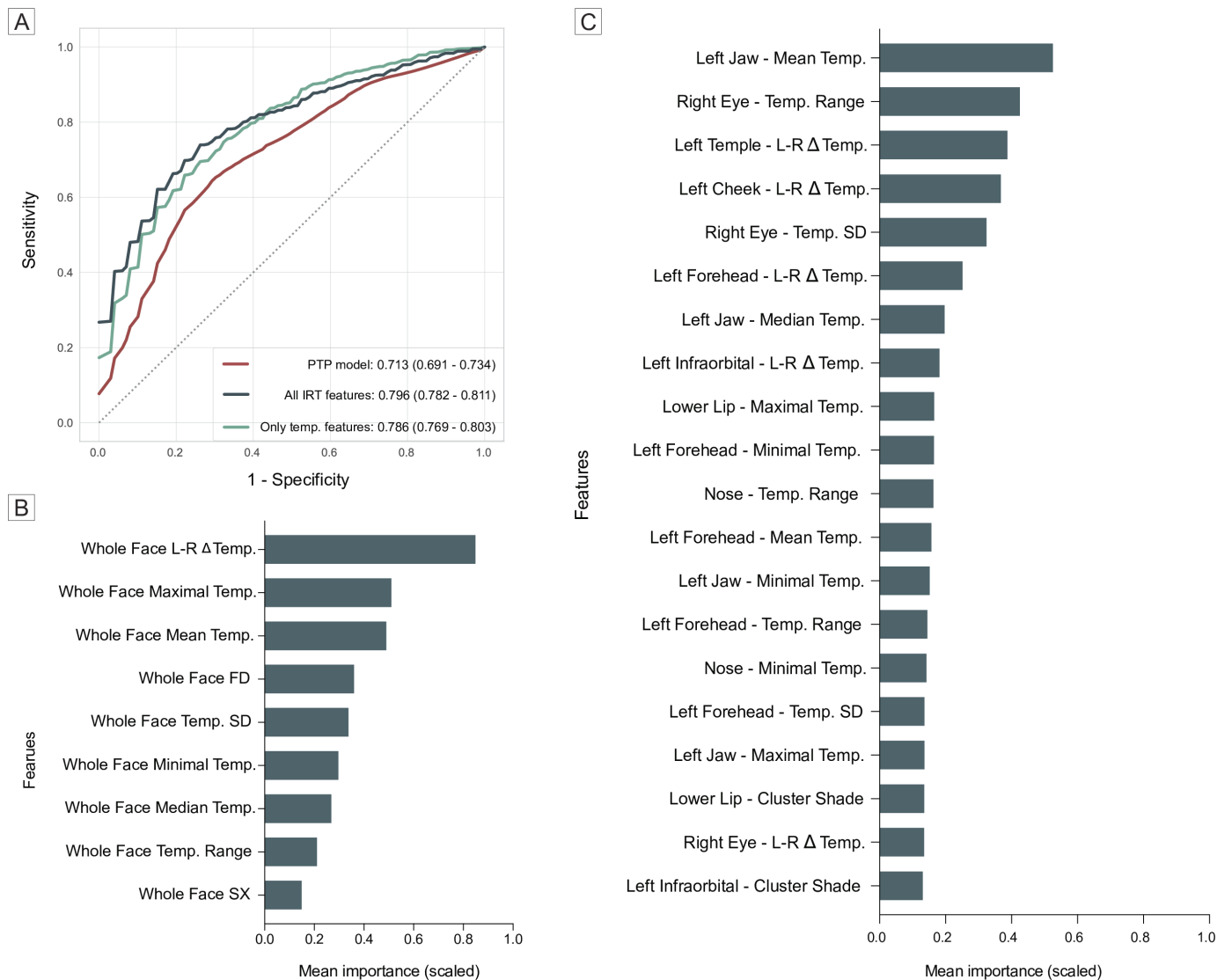


Figure 3 Analyses of the interpretable IRT features for coronary artery disease (CAD) prediction. (A) Predictive performance for using all or traditional temperature-only IRT features for CAD prediction, as compared with the PTP model; (B) the ranking of the scaled importance value of the whole-face level features; (C) the ranking of the scaled importance value of the top 20 region of interest-level features. FD, fractal dimension; IRT, infrared thermography; L-R Δ , left-right difference; PTP, pretest probability; SX, sum of extrema; Temp., temperature; Δ , value difference.

RESULTS

Study participant overview

Between 6 September 2021 and 10 February 2023, a total of 893 adult participants undergoing ICA or CCTA evaluation were screened. After excluding 433 individuals according to study criteria, 460 eligible participants were included. All participants underwent standard IRT filming, and their image quality was assessed, with all participants having at least one qualified IRT image, constituting the final analysis dataset (figure 1). Among this final dataset (460 participants with corresponding 460 IRT images), the mean age was 58.4 (SD 10.4) and 126 individuals (27.4%) were female. A total of 322 participants (70.0%) were confirmed to have CAD. Table 1 presents the baseline characteristics between CAD and non-CAD participants. Compared with non-CAD participants, those with CAD were older, more likely to be male,

had a greater prevalence of lifestyle, clinical and laboratory risk factors for CAD, as well as more frequent use of primary prevention medications.

CAD prediction model performance

The performance of the individual CAD prediction models in the validation sets under the current five-repeated fivefold cross-validation design is summarised in online supplemental table S3. In comparison to the guideline-recommended PTP model (AUC 0.713, 95% CI 0.691 to 0.734), the IRT image model exhibited a considerably higher performance (AUC 0.804, 95% CI 0.785 to 0.823). Furthermore, when integrating clinical variables from the PTP models with the IRT image as joint input, the resulting IRT-PTP hybrid model (AUC 0.805, 95% CI 0.793 to 0.827) did not yield a significant difference in

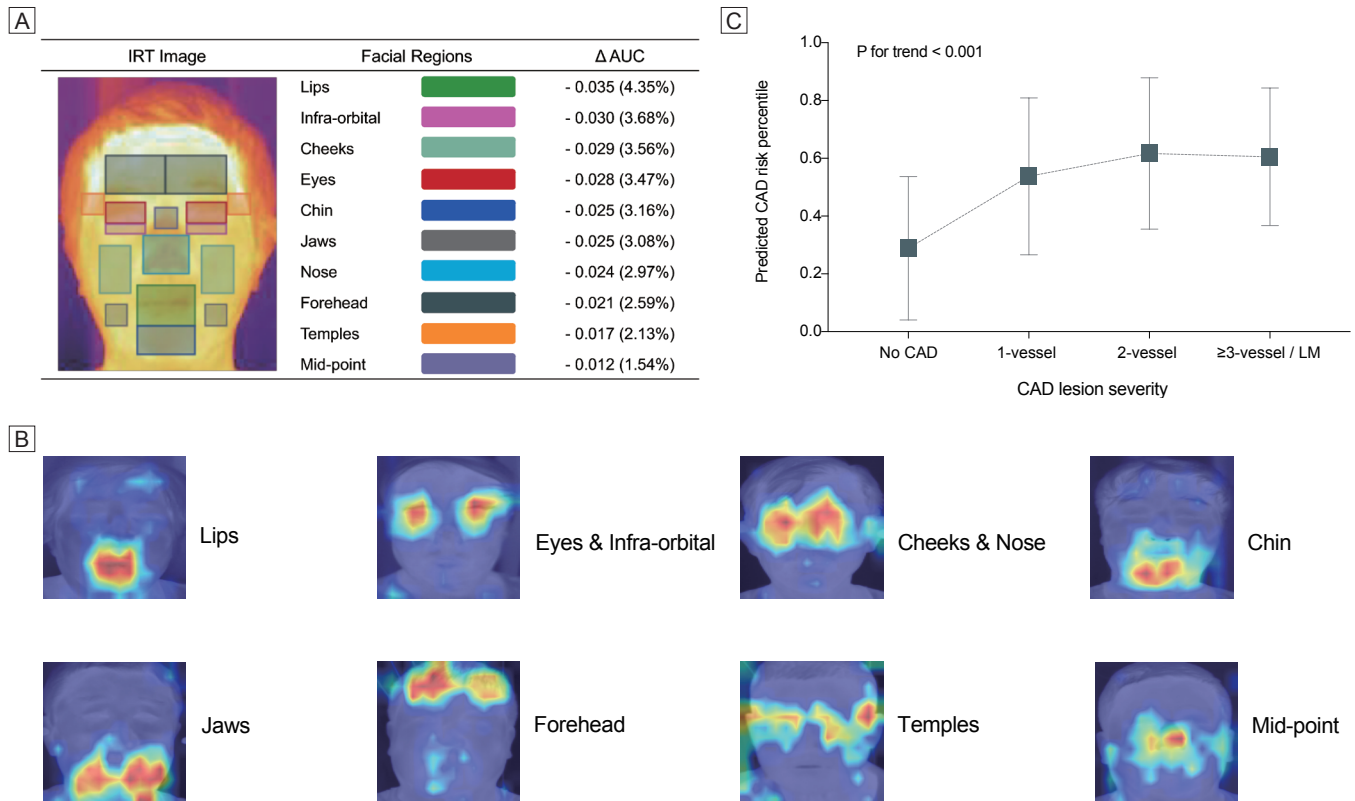


Figure 4 Interpretation and visualisation of the IRT image model. (A) Results of the occlusion tests in assessing the effect of individual facial regions after occlusion on the IRT image model's predictive performance, measured by the degree of AUC reduction (Δ AUC); (B) visualisation of examples with specific facial regions deemed important for IRT image model prediction highlighted by the Gradient-weighted Class Activation Map methods; (C) dose–response relationship between the CAD lesion severity and the IRT image model predicted CAD risk percentiles. AUC, area under the curve; CAD, coronary artery disease; IRT, infrared thermography; LM, left main.

performance improvement compared with the IRT image model alone (figure 2).

Interpretable IRT features for CAD prediction

Based on the manually extracted interpretable IRT features for further validation, both the all IRT feature approach (AUC 0.796, 95% CI 0.782 to 0.811) and the traditional temperature feature-only approach (AUC 0.786, 95% CI 0.769 to 0.803) demonstrated superior performance (figure 3A), which closely aligned with the performance of the end-to-end IRT image model in utilisation of IRT information for CAD prediction.

The relative importance rankings of the interpretable IRT features for CAD prediction are depicted in figure 3B,C. At the whole-face level (figure 3B), of the three most significant features, the most influential one was the overall left-right temperature difference, followed by the maximal facial temperature, mean facial temperature and fractal dimension of facial temperature. Among the three most influential ROI-specific features (figure 3C), the mean temperature of the left jaw region exhibited the highest impact, followed by the temperature range of the right eye region and the left-right temperature difference of the left temple regions.

Interpretation of the IRT image model

The occlusion experiments (figure 4A) demonstrated varying degrees of reduction in the IRT image model performance when occluding different ROIs for any of the 10 facial regions. The largest decrease was observed when occluding the upper and lower lips (ie, the oral and perioral) region (Δ AUC=−0.035, 4.35%), followed by the left and right infraorbital (Δ AUC=−0.030, 3.68%) and cheeks (Δ AUC=−0.029, 3.56%), etc. In addition, examples of facial regions in the IRT image deemed important for the IRT image model prediction were visualised using the Grad-CAM method (figure 4B). Moreover, a trend of higher predicted CAD risk percentile was observed as CAD severity increased (figure 4C).

Table 2 presents the potential of the modified IRT image model to predict various surrogate labels associated with CAD. For ASCVD traditional risk factors, the image model demonstrated good performance in identifying hyperlipidaemia (0.831, 95% CI 0.811 to 0.850), male sex (0.988, 95% CI 0.985 to 0.991), smoking (0.749, 95% CI 0.694 to 0.804), body mass index (mean absolute error (MAE) 2.593, 95% CI 2.147 to 3.038), HbA1C% (MAE 0.772, 95% CI 0.686 to 0.859), etc. Furthermore, the model also exhibited potential in identifying other cardiovascular (eg, NT-proBNP>300 pg/mL, 0.636

Table 2 IRT model prediction for surrogate labels contributing or related to CAD

Surrogate labels	AUC (95% CI)	MAE (95% CI)
ASCVD traditional risk factors		
Hyperlipidaemia	0.831 (0.811 to 0.850)	/
Hypertension	0.640 (0.607 to 0.673)	/
Diabetes mellitus	0.659 (0.573 to 0.745)	/
Male	0.988 (0.985 to 0.991)	/
Age	/	8.23 (7.543 to 8.914)
Body mass index	/	2.593 (2.147 to 3.038)
Smoking	0.749 (0.694 to 0.804)	/
Early ASCVD family history	0.691 (0.587 to 0.795)	/
HbA1C%	/	0.772 (0.686 to 0.859)
Inflammation and other cardiovascular markers		
Chronic inflammatory diseases	0.631 (0.536 to 0.726)	/
Elevated ESR level*	0.645 (0.524 to 0.766)	/
Elevated Inflammatory Markers [†]	0.601 (0.539 to 0.663)	/
NT-proBNP>300 pg/mL	0.636 (0.593 to 0.678)	/

*The elevated level refers to the laboratory value higher than the upper bound of reporting normal range.

[†]Inflammatory markers include ESR, C reactive protein and Interleukin-6.

ASCVD, atherosclerotic cardiovascular diseases; AUC, area under the curve; CAD, coronary artery disease; CRP, C reactive protein; ESR, erythrocyte sedimentation rate; HbA1C%, Hemoglobin A1C%; IRT, infrared thermography; MAE, mean absolute error; NT-proBNP, N-terminal pro-B-type natriuretic peptide.

(95% CI 0.593 to 0.678)) and inflammation-related labels (eg, chronic inflammatory diseases, 0.631 (95% CI 0.536 to 0.726), elevated erythrocyte sedimentation rate, 0.645 (95% CI 0.524 to 0.766), etc).

DISCUSSION

In this study, we have demonstrated the feasibility of using IRT temperature information from human faces to predict CAD in a non-contact manner. Our developed deep-learning IRT image model for CAD prediction achieved superior performance compared with the current guideline-recommended PTP model that relied on traditional risk factors and clinical presentation for CAD assessment. The current findings highlighted the promising potential of facial temperature information in CAD assessment, which could be harnessed through either the end-to-end IRT image-based deep-learning approach or through a more interpretable temperature variable approach in clinical practice (figure 5).

The feasibility of IRT information for CAD prediction was built on previous evidence between IRT and ASCVD-related conditions. For ASCVD risk factors, previous studies demonstrated that combining temperature and textural features from facial IRT images with clinical risk factors achieved high prediction accuracy for type II diabetes.¹⁴ Associations were also found between body surface temperature measured by IRT in specific regions and blood lipid levels.¹⁵ Distinct IRT distribution patterns, especially temperature asymmetry, have also been observed in individuals at high risk or with established

CAD.²⁹ Inflammation, an increasingly recognised non-traditional risk factor contributing to ASCVD,^{30–32} has also been reflected in IRT images in various chronic inflammatory conditions.^{17 18} Therefore, it is possible that IRT information reflective of inflammation activity could be used in ASCVD prediction and evaluation. The potential of IRT in assessing established ASCVD diseases has also been explored in previous studies, including PAD from IRT measurements in peripheral extremities¹³ and carotid atherosclerosis detected by IRT obtained from neck and facial regions.^{12 33} In addition, studies have also investigated the dynamic temperature changes captured through IRT to reflect vascular function, which was further shown to be well correlated with ASCVD risk, CAC score and myocardial perfusion defects.^{34–36} However, previous studies generally employed simplistic approaches for IRT information extraction and analysis, which could limit their ability to comprehensively and objectively integrate the full breadth of IRT information for disease assessment. In our study, we conducted surrogate label prediction experiments to replicate and validate these previous findings. The observed overall strong performance of our IRT models in predicting these CAD-related surrogate labels further strengthens the pathophysiological plausibility and validity of facial IRT information for CAD prediction.

Internal validity and interpretability were prioritised in establishing the feasibility of IRT models in predicting CAD in the current study. The IRT image model employed a state-of-the-art deep-learning framework, allowing for

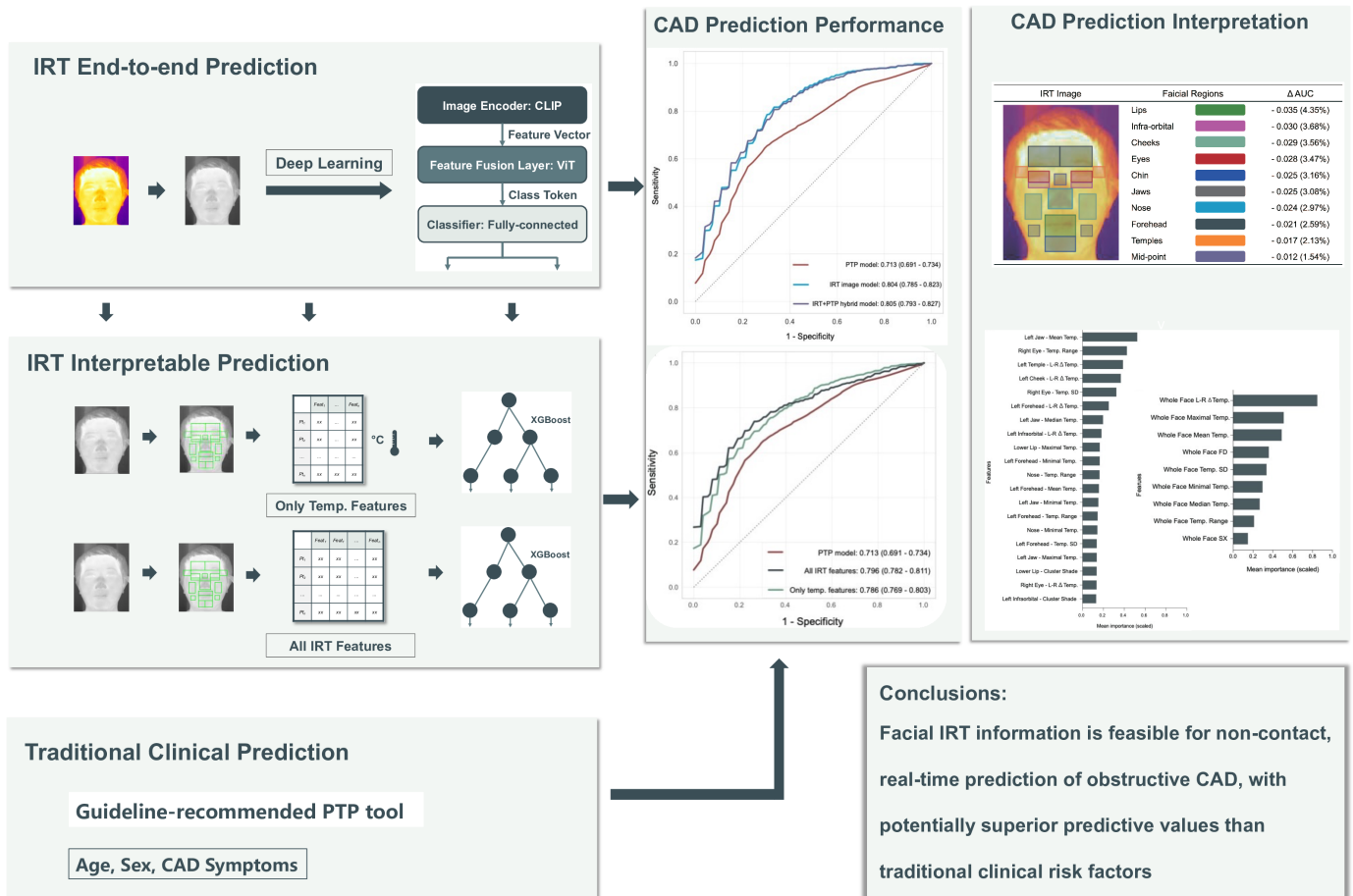


Figure 5 Central illustration. CAD, coronary artery disease; CLIP, contrastive language-image pretraining; FD fractal dimension; IRT, infrared thermography; L-R Δ, left-right difference; PTP, pretest probability; SX, sum of extrema; Temp., temperature; ViT, vision transformer; Δ, value difference.

robust extraction of high-fidelity image features and reliable prediction for our specific downstream task, even with a relatively small training sample size. Notably, the addition of clinical variables to the IRT image model did not yield further improvements compared with the stand-alone end-to-end IRT image-based approach, suggesting that the facial IRT information extracted by the algorithm may already encompass relevant clinical information associated with CAD. Model interpretation also confirmed that the deep-learning algorithm focused on potentially relevant facial IRT areas and helped identify important facial regions contributing to predictions. Furthermore, the observed dose–response relationship between predicted CAD risk and CAD severity further bolstered the model’s credibility. The predictive value of IRT information for CAD was further validated by the interpretable IRT tabular features, which could also avoid potential inclusion of irrelevant image details that might give away the prediction label and thus inflate performance.³⁷ Importantly, this interpretable IRT tabular feature-based approach demonstrated relatively consistent performance as the deep-learning IRT image model. With these human-interpretable IRT features, we also gained insights into specific aspects of facial IRT temperature information deemed important for the CAD predictions, with

prominent aspects such as facial temperature asymmetry and distribution non-uniformity.

The feasibility of IRT temperature-based CAD prediction suggests potential future applications and research opportunities. As a biophysiological-based health assessment modality, IRT provides disease-relevant information beyond traditional clinical measures that could enhance ASCVD and related chronic condition assessment. The non-contact, real-time nature of the end-to-end IRT image model allows for instant disease assessment at the point of care, which could streamline clinical workflows and save time for important physician–patient decision-making. In addition, it has the potential to enable mass prescreening for more cost-effective adoption of downstream screening modalities (eg, CAC score). Deploying IRT-based assessment in a non-contact and passive monitoring manner could also enable continuous evaluation of disease progression in the daily living spaces outside of regular clinic visits.³⁸ Depending on resource availability, the temperature-based CAD assessment could be adopted accordingly with satisfactory performance, from the more widely available traditional temperature features that could be measured with regular thermometer, to the end-to-end IRT-based imaging approach that uses validated IR cameras with good reproducibility and minimal operator

training. Importantly, IR temperature-based prediction tools have several inherent advantages that enhance their trustworthiness for healthcare providers, including its physiologically sound mechanism, high reproducibility and user-friendly operation.

Several limitations should be acknowledged in the current study. First, the relatively small sample size may have limited the performance of current IRT algorithms. To address this limitation, we employed ML algorithms with simplistic structure optimised for small-sample prediction tasks, which minimised the training requirements while still achieving valid and satisfactory performance. Second, the study was conducted in a single-centre cohort, necessitating external validation from diverse patient populations in multicentre studies. Lastly, the study participants were patients referred for confirmatory CAD examinations, and therefore, represented a higher PTP spectrum, which could limit the generalisability of current findings. Future research should include a broader spectrum of patients for CAD evaluation.

CONCLUSION

In this diagnostic study, we have examined and established the feasibility of using non-contact captured human facial temperature information by IRT in predicting CAD. Our developed IRT prediction models, based on advanced ML technology, have exhibited promising potential compared with the current conventional clinical tools. Further investigations incorporating larger sample sizes and diverse patient populations are needed to validate the external validity and generalisability of current findings.

Author affiliations

¹Department of Automation, Tsinghua University, Beijing, China

²Shenzhen International Graduate School, Tsinghua University, Shenzhen, Guangdong, China

³National Clinical Research Center of Cardiovascular Diseases, Fuwai Hospital, National Center for Cardiovascular Diseases, Beijing, China

⁴State Key Laboratory of Cardiovascular Disease, Fuwai Hospital, National Center for Cardiovascular Diseases, Beijing, China

⁵Chinese Academy of Medical Sciences and Peking Union Medical College, Beijing, China

⁶Department of Cardiovascular Surgery, Fuwai Hospital, National Center for Cardiovascular Diseases, Beijing, China

⁷Key Laboratory of Coronary Heart Disease Risk Prediction and Precision Therapy, Chinese Academy of Medical Sciences and Peking Union Medical College, Beijing, China

⁸Beijing National Research Center for Information Science and Technology (BNRist), Tsinghua University, Beijing, China

Acknowledgements We thank Yue Zhang for her assistance with patient enrolment and logistics, and all participating staff members in the catheterisation laboratory and the radiology department for their assistance in the collection and interpretation of ICA and CCTA.

Contributors ZZ, XJ and SL conceived the overall study. JZ and SL designed the experiments. JZ, RS, SL, SY, XL and YZ performed the data acquisition, extracting and cleaning. MK, JZ and XY performed the data processing and conducted the experiments. MK, XY, CL and MS designed and implemented the algorithm. JZ, MK and XS analysed the data. ZZ and XJ directed the project. All authors contributed to the interpretation of the results and JZ drafted the final manuscript, which was reviewed, revised and approved by all authors. ZZ is the guarantor of this study.

Funding This work was supported by grants from the National High Level Hospital Clinical Research Funding of Fuwai Hospital, Chinese Academy of Medical Sciences (2022-GSP-GG-28 to ZZ, 2022-GSP-QN-10 and 2023-GSP-RC-10 to SL), the National Natural Science Foundation of China (Key Programme; 81830072 to ZZ), and the National Natural Science Foundation of China (61827804 and 62131011 to XJ).

Disclaimer The funders had no role in study design, data collection, data analysis, data interpretation, writing of the report or the decision to submit the paper for publication.

Competing interests None declared.

Patient consent for publication Not applicable.

Ethics approval This study involves human participants and was approved by name of the ethics committee: Ethics Committee of Fuwai Hospital, CAMS and PUMC, reference number of ethics approval: 2021-1471. Participants gave informed consent to participate in the study before taking part.

Provenance and peer review Not commissioned; internally peer reviewed.

Data availability statement Data are available on reasonable request. The data collected and analysed in the current study cannot be shared publicly due to patient privacy. All data were approved for research purposes in Fuwai hospital only. Any external use requires additional consent and ethical approval from Fuwai hospital institutional review board and may be available from the corresponding author on reasonable request.

Supplemental material This content has been supplied by the author(s). It has not been vetted by BMJ Publishing Group Limited (BMJ) and may not have been peer-reviewed. Any opinions or recommendations discussed are solely those of the author(s) and are not endorsed by BMJ. BMJ disclaims all liability and responsibility arising from any reliance placed on the content. Where the content includes any translated material, BMJ does not warrant the accuracy and reliability of the translations (including but not limited to local regulations, clinical guidelines, terminology, drug names and drug dosages), and is not responsible for any error and/or omissions arising from translation and adaptation or otherwise.

Open access This is an open access article distributed in accordance with the Creative Commons Attribution Non Commercial (CC BY-NC 4.0) license, which permits others to distribute, remix, adapt, build upon this work non-commercially, and license their derivative works on different terms, provided the original work is properly cited, appropriate credit is given, any changes made indicated, and the use is non-commercial. See: <http://creativecommons.org/licenses/by-nc/4.0/>.

ORCID iDs

Juntong Zeng <http://orcid.org/0000-0003-1235-3180>

Zhe Zheng <http://orcid.org/0000-0002-9162-6492>

REFERENCES

- Vos T, Lim SS, Abbafati C, *et al*. Global burden of 369 diseases and injuries in 204 countries and territories, 1990-2019: a systematic analysis for the global burden of disease study 2019. *Lancet* 2020;396:1204-22.
- Fihn SD, Blankenship JC, Alexander KP, *et al*. 2014 ACC/AHA/AATS/PCNA/SCAI/STS focused update of the guideline for the diagnosis and management of patients with stable ischemic heart disease: a report of the American college of cardiology/American heart association task force on practice guidelines, and the American association for thoracic surgery, preventive cardiovascular nurses association, society for cardiovascular angiography and interventions, and society of thoracic surgeons. *J Am Coll Cardiol* 2014;64:1929-49.
- Knuuti J, Wijns W, Saraste A, *et al*. 2019 ESC guidelines for the diagnosis and management of chronic coronary syndromes. *Eur Heart J* 2020;41:407-77.
- Juarez-Orozco LE, Saraste A, Capodanno D, *et al*. Impact of a decreasing pre-test probability on the performance of diagnostic tests for coronary artery disease. *Eur Heart J Cardiovasc Imaging* 2019;20:1198-207.
- Cheng VY, Berman DS, Rozanski A, *et al*. Performance of the traditional age, sex, and angina typicality-based approach for estimating pretest probability of angiographically significant coronary artery disease in patients undergoing coronary computed tomographic angiography: results from the multinational coronary CT angiography evaluation for clinical outcomes: an international multicenter registry (CONFIRM). *Circulation* 2011;124:2423-32.

- 6 Genders TSS, Steyerberg EW, Hunink MGM, *et al.* Prediction model to estimate presence of coronary artery disease: retrospective pooled analysis of existing cohorts. *BMJ* 2012;344:e3485.
- 7 Reeh J, Therning CB, Heitmann M, *et al.* Prediction of obstructive coronary artery disease and prognosis in patients with suspected stable angina. *Eur Heart J* 2019;40:1426–35.
- 8 Fordyce CB, Douglas PS, Roberts RS, *et al.* Identification of patients with stable chest pain deriving minimal value from noninvasive testing: the PROMISE minimal-risk tool, a secondary analysis of a randomized clinical trial. *JAMA Cardiol* 2017;2:400–8.
- 9 Budoff MJ, Mayrhofer T, Ferencik M, *et al.* Prognostic value of coronary artery calcium in the PROMISE study (prospective multicenter imaging study for evaluation of chest pain). *Circulation* 2017;136:1993–2005.
- 10 Villines TC, Hulten EA, Shaw LJ, *et al.* Prevalence and severity of coronary artery disease and adverse events among symptomatic patients with coronary artery calcification scores of zero undergoing coronary computed tomography angiography: results from the CONFIRM (coronary CT angiography evaluation for clinical outcomes: an international multicenter) registry. *J Am Coll Cardiol* 2011;58:2533–40.
- 11 Tattersall GJ. Infrared thermography: a non-invasive window into thermal physiology. *Comp Biochem Physiol A Mol Integr Physiol* 2016;202:78–98.
- 12 Saxena A, Ng EYK, Lim ST. Infrared (IR) thermography as a potential screening modality for carotid artery stenosis. *Comput Biol Med* 2019;113:103419.
- 13 Piva G, Crepaldi A, Zenunaj G, *et al.* The value of infrared thermography to assess foot and limb perfusion in relation to medical, surgical, exercise or pharmacological interventions in peripheral artery disease: a systematic review. *Diagnostics (Basel)* 2022;12:12.
- 14 Thirunavukkarasu U, Umapathy S, Janardhanan K, *et al.* A computer aided diagnostic method for the evaluation of type II diabetes mellitus in facial thermograms. *Phys Eng Sci Med* 2020;43:871–88.
- 15 Thiruvengadam J, Anburajan M, Menaka M, *et al.* Potential of thermal imaging as a tool for prediction of cardiovascular disease. *J Med Phys* 2014;39:98–105.
- 16 Gao M-J, Xue H-Z, Cai R, *et al.* A preliminary study on infrared thermograph of metabolic syndrome. *Front Endocrinol (Lausanne)* 2022;13:851369.
- 17 Pauk J, Ihnatouski M, Wasilewska A. Detection of inflammation from finger temperature profile in rheumatoid arthritis. *Med Biol Eng Comput* 2019;57:2629–39.
- 18 Schiavon G, Capone G, Frize M, *et al.* Infrared thermography for the evaluation of inflammatory and degenerative joint diseases: a systematic review. *Cartilage* 2021;13:1790S–1801S.
- 19 Christoffersen M, Frikke-Schmidt R, Schnohr P, *et al.* Visible age-related signs and risk of ischemic heart disease in the general population: a prospective cohort study. *Circulation* 2014;129:990–8.
- 20 Lin S, Li Z, Fu B, *et al.* Feasibility of using deep learning to detect coronary artery disease based on facial photo. *Eur Heart J* 2020;41:4400–11.
- 21 Topol EJ. High-performance medicine: the convergence of human and artificial intelligence. *Nat Med* 2019;25:44–56.
- 22 Zeng J, Shao J, Lin S, *et al.* Optimizing the dynamic treatment regime of in-hospital warfarin anticoagulation in patients after surgical valve replacement using reinforcement learning. *J Am Med Inform Assoc* 2022;29:1722–32.
- 23 Johnson KW, Torres Soto J, Glicksberg BS, *et al.* Artificial intelligence in cardiology. *J Am Coll Cardiol* 2018;71:2668–79.
- 24 Collins GS, Reitsma JB, Altman DG, *et al.* Transparent reporting of a multivariable prediction model for individual prognosis or diagnosis (TRIPOD): the TRIPOD statement. *BMJ* 2015;350:g7594.
- 25 Radford A, Kim JW, Hallacy C, *et al.* Learning transferable visual models from natural language supervision. 2021. 8748–63. Available: <https://proceedings.mlr.press/v139/radford21a.html> [accessed 14 Jun 2023]
- 26 Dosovitskiy A, Beyer L, Kolesnikov A, *et al.* An image is worth 16X16 words: transformers for image recognition at scale. *Arxiv* 2020.
- 27 Selvaraju RR, Cogswell M, Das A, *et al.* Grad-CAM: visual explanations from deep networks via gradient-based localization. *Int J Comput Vis* 2020;128:336–59.
- 28 Chen T, Guestrin C. Xgboost: a scalable tree boosting system. Proceedings of the ACM SIGKDD international conference on knowledge discovery and data mining; 2016:785–94.
- 29 Choda G, Rao G. Thermal imaging for the diagnosis of early vascular dysfunctions: a case report. 2020.
- 30 Kaptoge S, Di Angelantonio E, Lowe G, *et al.* C-reactive protein concentration and risk of coronary heart disease, stroke, and mortality: an individual participant meta-analysis. *Lancet* 2010;375:132–40.
- 31 Pai JK, Pischon T, Ma J, *et al.* Inflammatory markers and the risk of coronary heart disease in men and women. *N Engl J Med* 2004;351:2599–610.
- 32 Ridker PM, Hennekens CH, Buring JE, *et al.* C-reactive protein and other markers of inflammation in the prediction of cardiovascular disease in women. *N Engl J Med* 2000;342:836–43.
- 33 Yang Y, Liu J. Detection of atherosclerosis through mapping skin temperature variation caused by carotid atherosclerosis plaques. *J Therm Sci Eng Appl* 2011;3.
- 34 Gul KM, Ahmadi N, Wang Z, *et al.* Digital thermal monitoring of vascular function: a novel tool to improve cardiovascular risk assessment. *Vasc Med* 2009;14:143–8.
- 35 Ahmadi N, Hajsadeghi F, Gul K, *et al.* Relations between digital thermal monitoring of vascular function, the framingham risk score, and coronary artery calcium score. *J Cardiovasc Comput Tomogr* 2008;2:382–8.
- 36 Ahmadi N, Usman N, Shim J, *et al.* Vascular dysfunction measured by fingertip thermal monitoring is associated with the extent of myocardial perfusion defect. *J Nucl Cardiol* 2009;16:431–9.
- 37 Zech JR, Badgeley MA, Liu M, *et al.* Confounding variables can degrade generalization performance of radiological deep learning models. *PLoS Med* 2018;15:11.
- 38 Haque A, Milstein A, Fei-Fei L. Illuminating the dark spaces of Healthcare with ambient intelligence. *Nature* 2020;585:193–202.